

Synthesis of Ethylene Terephthalate and Ethylene Naphthalate (PET-PEN) Block-co-Polyesters with Defined Surface Qualities by Tailoring Segment Composition

Björn Geyer,¹ Stefan Röhner,¹ Günter Lorenz,^{1,2} Andreas Kandelbauer^{1,2}

¹Reutlingen Research Institute (RRI), Reutlingen University, Alteburgstrasse 150, 72762 Reutlingen, Germany

²School of Applied Chemistry, Reutlingen University, Alteburgstrasse 150, 72762 Reutlingen, Germany

Correspondence to: A. Kandelbauer (E-mail: andreas.kandelbauer@reutlingen-university.de)

ABSTRACT: Ethylene terephthalate and ethylene naphthalate oligomers of defined degree of polymerization were synthesized via chemical recycling of the parent polymers. The oligomers were used as defined building blocks for the preparation of novel block-co-polyesters having tailored sequence compositions. The sequence lengths were systematically varied using Design of Experiments. The dispersive surface energy and the specific desorption energy of the co-polymers were determined by inverse gas chromatography. The study shows that polyethylene terephthalate-polyethylene naphthalate (PET-PEN) block-co-polyesters of defined sequence lengths can be prepared. Furthermore, the specific and dispersive surface energies of the obtained block-co-polyesters showed a linear dependence on the oligomer molecular weight and it was possible to regulate and control their interfacial properties. In contrast, with the corresponding random-block-co-polyesters no such dependence was found. The synthesized block-co-polyesters could be used as polymeric modifying agents for stabilizing PET-PEN polymer blends. © 2014 Wiley Periodicals, Inc. *J. Appl. Polym. Sci.* **2014**, *131*, 40731.

KEYWORDS: compatibilization; polyesters; recycling; synthesis and processing; thermoplastics

Received 5 December 2013; accepted 18 March 2014

DOI: 10.1002/app.40731

INTRODUCTION

Polymer blends represent important key engineering materials due to the wide range of technological performance profiles that can be adjusted by proper selection of blending components and functional fillers.^{1–9} Even by suitable combination of commodity polymers and incorporation of organic or inorganic particles the properties of polymer blends can be improved and their performance specifications can be extended at reasonable costs.^{10,11} Fillers such as layered silicates or carbon nanotubes are applied to increase mechanical or barrier properties of polymers. To achieve homogenous distribution and ideal embedding of such functional fillers, the interfacial properties of the polymer matrix have to be adapted to ensure optimal performance.^{12–15}

Blends of two polymeric systems are often used as packaging or laminating materials. An important example is the use of polyethylene terephthalate-polyethylene naphthalate (PET-PEN) blends as encapsulating materials for solar cells.^{16–18} PET-PEN blends have excellent mechanical properties and better barrier properties than pure PET.¹⁶ However, PET and PEN are generally regarded as immiscible^{16,19} and their blends tend to segregate. They often lead to opaque products and are problematic in

applications where excellent optical appearance and optical transparency of the products is demanded. Therefore, PET-PEN blends need to be stabilized to prevent phase separation. Compatibilization of PET-PEN blends can be accomplished by addition of suitable adhesion promoters. Good adhesion promoters should be chemically very similar to the blending components and, hence, PET-PEN block-co-polyesters could represent an ideal material.

Although numerous attempts have been made to prepare PET-PEN block-co-polyesters,^{20–24} to our knowledge so far, no study has been published where (a) PET-PEN block-co-polyesters of defined sequence lengths have been rationally synthesized and (b) the sequence lengths of PET-PEN block-co-polyesters were systematically varied to arrive at defined polymer properties.

In this study, the synthesis of a series of novel PET-PEN block-co-polyesters based on defined PET and PEN oligomer units is described and their interfacial properties are studied by inverse gas chromatography (IGC).²⁵ The presented approach is based on the chemical recycling of PET and PEN to oligomers of defined molecular weight as tailored building blocks for block-co-polyesters of defined segment dimensions.

Table I. Calculation of the Degree of Polymerization in Dependence of the Used Mass of Adipic Acid

Sample	Oligomer	Mass of PEN (g)	Mass of adipic acid (g)	Calculated DP ^a
O1	PEN5	25.60	3.56	5
O2	PEN10	25.57	1.64	10
O3	PEN20	25.66	0.80	20
O4	PEN40	25.60	0.39	40
O5	PEN80	25.59	0.20	78
O6	PEN160	25.57	0.10	158

^aDP calculated according to Geyer et al.²⁶

In a first step, tailored oligomers of ethylene naphthalate and terephthalate were prepared by the degradation of the parent polymers with adipic acid. Subsequently, block-*co*-polyesters of defined composition of ethylene terephthalate and ethylene naphthalate units were generated. To test the hypothesis that the interfacial properties of the block-*co*-polyesters can be tuned by defining the segment lengths, random-*co*-polyesters were also synthesized from the same raw materials for comparison. By determination of the dispersive surface energy and the specific desorption energy of both *co*-polyester types, response surface models (RSMs) were calculated to quantify the individually adjustable surface properties in dependence of the block length composition.

EXPERIMENTAL

Chemicals

Polyethylene naphthalate (PEN ES 366300) with an average molecular weight of 55195 g mol⁻¹, was supplied by Goodfellow (Huntingdon, UK). The degrading agent used for preparation of oligomeric PEN fragments of defined chain lengths was adipic acid, which was purchased from Acros Organics (Geel, Belgium). Oligomeric ethylene terephthalate with different degrees of polymerization was used for the synthesis of block-*co*-polyesters with the PEN fragments. The oligomeric ethylene terephthalate building blocks were prepared from PET (Arnite® A04 900, procured from DSM Unlimited, Sittard, the Netherlands) by controlled depolymerization using chain scission agents at various stoichiometric ratios as described in Geyer et al.²⁶

For IGC, *n*-hexane, *n*-heptane, *n*-octane, and *n*-nonane were used as non-polar probes. The polar probe molecules were chloroform, acetone, 1,4-dioxane, ethyl acetate, and 1-butanol. Methane was used as the non-interacting probe for determination of the dead time. All probes were of analytical grade and were purchased from Th. Geyer, Renningen, Germany.

Methods

Synthesis of Oligomers. Preparation of oligomeric ethylene naphthalate and terephthalate was performed by controlled depolymerization of the corresponding PEN and PET polymers. Controlled depolymerization was achieved with adipic acid as the chain scission reagent according to the method described in a previous article.²⁶ To generate different degrees of polymeriza-

tion, PEN was mixed with different stoichiometric amounts of adipic acid in the melt under nitrogen atmosphere for 2 h (Table I). Herein, the mass of adipic acid was calculated according to eq. (1), where $\bar{M}_{\text{Oligomer}}$ is the molecular mass of the desired oligomer, M_A is the molecular mass of adipic acid and m_{PEN} , m_A are the masses of used PEN and adipic acid.

$$\bar{M}_{\text{Oligomer}} = \frac{m_{\text{PEN}}}{m_A} \cdot M_A + M_A \quad (1)$$

PET oligomers of degrees of polymerization 5, 20, and 40 were produced in an analogous way.²⁶ The resulting oligomers were named after the used parent polymer using the degree of polymerization (DP) as suffix. For example, a PEN oligomer of DP 20 is called PEN20.

Synthesis of Block-*co*-Polyesters of Defined Block Lengths and Random-*co*-Polyesters Designed from Oligomeric PEN and PET. Block-*co*-polyesters comprising ethylene naphthalate and ethylene terephthalate segments of defined sequence lengths were prepared by combining oligomers from PEN and PET. Different combinations of oligomeric PEN and PET of degrees of polymerization 5, 20, and 40 were melt-mixed under nitrogen atmosphere in a molar ratio of 1 : 1 for 5 min according to the factorial experimental design summarized in Table II.

The same compositions of PET- and PEN oligomers were mixed in the melt under nitrogen atmosphere for 20 min to generate random-*co*-polyesters as reference materials (Table II). After cooling to room temperature under nitrogen atmosphere, samples were pulverized with an IKA A 10 analytical mill for sequence length determination.

The resulting block-*co*-polyesters were named after the used oligomer fragments. For example, the block-*co*-polymer that was prepared from PET oligomer with a DP of 20 reacted with a PEN oligomer of DP of 20 was named PET20PEN20. Random-*co*-polymers were labeled “rand.”

¹H-NMR Spectroscopic Analysis. Determination of the obtained degrees of polymerization in PEN oligomers and of the sequence lengths in the PET-PEN *co*-polyesters was done by ¹H-NMR spectroscopy.^{27–30} All NMR-spectra were recorded on a Bruker AC 250 NMR spectrometer at a magnetic field strength of 5.85 T (250.10 MHz for ¹H NMR) at 27°C (University of Tübingen, Germany). The ¹H 90° pulse length was 9.6 μs, the spectral width was 4000 Hz. Samples were dissolved in a solution of deuterio trifluoroacetic acid and deuterio chloroform (1 : 1, v/v). Chemical shifts were reported relative to the residual proton of deuterio chloroform at 7.27 parts per million (ppm).

Determination of the Interfacial Properties of *co*-Polyesters from PEN- and PET-Oligomers. As characteristic surface properties of the different *co*-polyester specimens, the dispersive surface energy and the specific desorption energy of the *co*-polyester samples were determined by IGC. An Agilent 6890 Series Gas Chromatograph with flame ionization detector and Chemstation control software version 1.5 (Porotec GmbH, Hofheim/Ts., Germany) was used. The resulting data was treated with IGC analysis software version 1.1 from Surface

Table II. Factorial Experimental Design for the Syntheses of Block- and Random-*co*-Polyesters

Sample	Co-polymer	Co-polymer type	Degree of polymerization		Mass (g)		Mixing time (Min)
			PET	PEN	PET	PEN	
P1	PET5PEN5	Block	5	5	5.10	6.00	5
P2	PET40PEN40	Block	40	40	4.95	6.00	5
P3	PET40PEN5	Block	40	5	6.00	1.00	5
P4	PET5PEN40	Block	5	40	0.63	6.00	5
P5	PET20PEN20	Block	20	20	4.67	6.00	5
P6	PET5PEN5rand	Random	5	5	5.10	6.00	20
P7	PET40PEN40rand	Random	40	40	4.95	6.00	20
P8	PET40PEN5rand	Random	40	5	6.00	1.00	20
P9	PET5PEN40rand	Random	5	40	0.63	6.00	20
P10	PET20PEN20rand	Random	20	20	4.67	6.00	20

measurements Systems (Alperton, Middlesex, London, UK). Helium was used as carrier gas with a flow rate of $20 \text{ cm}^3 \text{ min}^{-1}$.

Samples were grinded and sieved [60 mesh (US), (250 μm)] for surface characterization. For this purpose, each sample (0.1 g) was mixed with inert glass beads (size 0.25 – 0.5 mm) to prevent column blocking and packed in silanized glass columns (length 0.3 m) with an internal diameter of 3 mm. The columns were plugged at both ends with silanized glass wool. The samples were conditioned at 35°C (308 K) and 0% relative humidity for 12 h under a helium flow of $20 \text{ cm}^3 \text{ min}^{-1}$. The unpolar probes (*n*-hexane, *n*-heptane, *n*-octane, and *n*-nonane) were injected at a partial pressure of $0.05 p/p_0$ to assure infinite dilution. Determination of the dead time volume was conducted by injection of methane at a partial pressure of $0.01 p/p_0$. The values for the dispersive surface energy, γ_S^D , of all *co*-polyester samples were determined from the net retention volumes of the homologous series of *n*-alkanes according to the method described by Schultz and Lavielle.³¹ This approach is briefly summarized in eq. (2), where V_N is the net-retention volume, N_A is Avogadro's number, a is the probe surface area, γ_L^D is the dispersive component of the surface tension of the liquid probe molecule and a reference state dependent constant C . γ_S^D was obtained from the slope of the plot of $RT \ln V_N$ against $a(\gamma_L^D)^{\frac{1}{2}}$ [eq. (2)].

$$RT \ln V_N = 2N_A (\gamma_S^D)^{\frac{1}{2}} a (\gamma_L^D)^{\frac{1}{2}} + C \quad (2)$$

The specific energy of desorption, ΔG_{sp} , was calculated as the vertical difference between the free enthalpy of desorption ($RT \ln V_N$) of the polar probe molecules (acetone, ethyl acetate, 1,4-dioxane, chloroform, and 1-butanol) and the free enthalpy of desorption of the reference line of the *n*-alkane series [$RT \ln V_N^{ref}$, eq. (3)].³¹

$$\Delta G_{sp} = RT \ln V_N - RT \ln V_N^{ref} \quad (3)$$

Lewis acid and base characteristics of block- and random-*co*-polyester samples were calculated as the ratio of the specific

desorption energies ΔG_{sp} of 1,4-dioxane and chloroform. This ratio indicates an acidic ($\frac{\Delta G_{sp}(\text{Dioxane})}{\Delta G_{sp}(\text{Chloroform})} \geq 1.1$) or basic character ($\frac{\Delta G_{sp}(\text{Dioxane})}{\Delta G_{sp}(\text{Chloroform})} \leq 0.9$) of the solid surface.³²

Infrared-Spectroscopy. Infrared spectroscopy was used to obtain a general overview of the structural changes in the original PEN upon degradation to oligomeric PEN samples. KBr-pellets were prepared from all PEN samples. Infrared spectra were recorded in transmission before and after PEN degradation using a Spectrum One (Perkin Elmer LAS GmbH, Rodgau-Jüdisheim, Germany). Each sample was measured within a wavenumber range between 4000 and 450 cm^{-1} .

Differential Scanning Calorimetry (DSC). The melting and crystallization temperatures and phase transition enthalpies of the prepared PET and PEN oligomers were determined by DSC. The glass transition temperatures of the synthesized *co*-polyester samples were also measured by DSC. DSC measurements were performed on a DSC 204 F1 Phoenix (Netzsch GmbH; Selb, Germany). Samples of 10 mg were weighed into aluminum crucibles (40 μL) with pierced lid and subjected to a dynamic temperature program (heating rate: 20 K min^{-1} , temperature range from 20 to 300°C) under nitrogen atmosphere. The obtained thermograms were treated using Netzsch Proteus – Thermal Analysis Version 4.8.3.

Experimental Design and Response Surface Analysis. An experimental design was performed to describe quantitatively the influence of block-*co*-polyester composition on the surface properties. A full factorial experimental design where two factors were varied at two levels was augmented by several replications of the center point. The factors varied were the sequence lengths of the ethylene naphthalate and ethylene terephthalate units of the block-*co*-polyesters; the sequence lengths were varied at three levels (5, 20, and 40). As the target responses, the dispersive surface energy γ_S^D and the specific desorption energy ΔG_{sp} were measured by IGC.

The center point experiment was repeated three times. To account for potential variations of the experimental error in

dependence on the position of the experiment in the experimental space, all factorial experiments were repeated twice. Overall, 22 different block-*co*-polyesters were synthesized within the experimental design. The computer software program Design Expert 7.0.0 (Stat-Ease, Minneapolis, Minnesota USA) was used to statistically analyze the experiments and to generate a RSM from the experimental data.

$x_i y$ A linear regression model of the form eq. (4) was generated.³³

$$y = \beta_0 + \sum_{i=1}^k \beta_i x_i + \varepsilon \quad (4)$$

In this equation, β_i are the regression coefficients to be determined, x_i are the main effects and ε is the experimental error occurring during a measurement. For the determination of all regression coefficients at least $n = 1 + \sum_{i=1}^k i$ experiments have to be carried out at the selected number of levels of the factors x_i . Thus, one obtains n equations of the form (5):^{34,35}

$$\begin{aligned} y_1 &= \beta_0 + \beta_1 x_{11} + \dots + \beta_k x_{1k} + \varepsilon_1 \\ y_2 &= \beta_0 + \beta_1 x_{21} + \dots + \beta_k x_{2k} + \varepsilon_2 \\ &\vdots \\ y_n &= \beta_0 + \beta_1 x_{n1} + \dots + \beta_k x_{nk} + \varepsilon_n \end{aligned} \quad (5)$$

For convenience, (5) can be written in matrix formulation as follows:

$$\vec{y} = X \cdot \vec{\beta} + \vec{\varepsilon} \quad (6)$$

In eq. (6), \vec{y} is the response vector of all n measurements, X is the matrix of explanatory variables at all levels, $\vec{\beta}$ is the vector of all regression coefficients and $\vec{\varepsilon}$ is the error vector (7).

$$\vec{y} = \begin{pmatrix} y_1 \\ \vdots \\ y_n \end{pmatrix}, X = \begin{pmatrix} 1 & x_{11} & x_{12} & \dots & x_{1k} \\ 1 & x_{21} & x_{22} & \dots & x_{2k} \\ \vdots & \vdots & \vdots & \ddots & \vdots \\ 1 & x_{n1} & x_{n2} & \dots & x_{nk} \end{pmatrix}, \vec{\varepsilon} = \begin{pmatrix} \varepsilon_1 \\ \vdots \\ \varepsilon_n \end{pmatrix} \quad (7)$$

Equation (6) is solved by the "least-squares"-method and $\vec{\beta}$ is calculated by eq. (8):³⁶

$$\vec{\beta} = (X^T X)^{-1} X^T \cdot \vec{y} \quad (8)$$

Using the calculated regression coefficients, β_i , and eq. (4), the response variable, y , can be calculated in dependence of the explanatory variables x_i .³⁵

RESULTS AND DISCUSSION

Preparation and Spectroscopic Characterization of Ethylene Naphthalate Oligomers

Oligomeric ethylene naphthalate was produced by melt-mixing PEN with varying concentrations of adipic acid under nitrogen

atmosphere for 2 h (Table I). In Figure 1, the chemical structure of the partially degraded and adipic acid modified PEN chain is given together with the corresponding 1H NMR spectrum of a typical oligomer sample. The positions of the protons used for NMR analysis are indicated in the chemical structure.

The DP was determined from the ratio between the peak integrals of the aliphatic ethylene protons (Figure 1, H4) of the PEN repeating units and the β -protons of adipic acid (Figure 1, protons labeled B) [eq. (9)]. The chemical shifts of all samples are listed in Table III.

The ratio of integrated peaks at a chemical shift of 1.76 ppm (peaks designated as "B" in Figure 1, representing the protons of adipic acid in β -position) and the integrated peaks at a chemical shift of 4.95, 4.75, and 4.63 ppm (peaks designated as "H4" in Figure 1) was calculated and yielded the DP of the degraded products according to eq. (9). As seen in Figure 1, the three peaks observed at chemical shifts 4.95, 4.75, and 4.63 ppm represent the four aliphatic protons of an ethylene bridging in a PEN-molecule corresponding to 4n protons in a PEN polymer chain.

$$DP = \frac{H4}{B} \quad (9)$$

By multiplying the obtained DP with the molecular mass of the repeating unit of PEN (242.23 g Mol⁻¹), the corresponding number-average of molecular weight was calculated for each sample [eq. (10)].

$$\overline{M}_n = 242.23 \text{ g} \cdot \text{Mol}^{-1} \cdot DP \quad (10)$$

As seen in Table III, the degrees of polymerization determined experimentally were in good agreement with the values calculated from stoichiometry. This shows that controlled degradation of the parent PEN polymer had taken place. It shows further that the use of a scission agent like adipic acid provides a valuable tool for synthesizing oligomeric fragments of defined molecular weight from a polymeric starting material. The successful use of chain scission agents to direct the depolymerization of PET was described earlier.²⁶

The qualitative changes in molecular structure upon degradation of PEN to oligomers were further studied by infrared spectroscopy. IR spectra were recorded from all adipic acid treated samples including the original PEN and the changes in absorbance patterns were analyzed as a result of the controlled degradation of PEN to defined oligomers. Figure 2 shows the infrared spectrum of the PEN parent polymer with its characteristic absorbance bands. Band assignments to functional groups of the PEN parent polymer are listed in Table IV.^{37,38} The absorbances of typical bonds and functional groups of PEN were compared with those of the oligomeric samples.

In the range from 2750 to 3750 cm⁻¹ the absorbances of hydroxyl-groups (3542 cm⁻¹) and ethylene-bridges (2963 and 2899 cm⁻¹) lost considerably in intensity upon adipic acid treatment, indicating the reduction of the number of hydroxyl-functionalities and ethylene bridges in PEN (Figure 3). This can

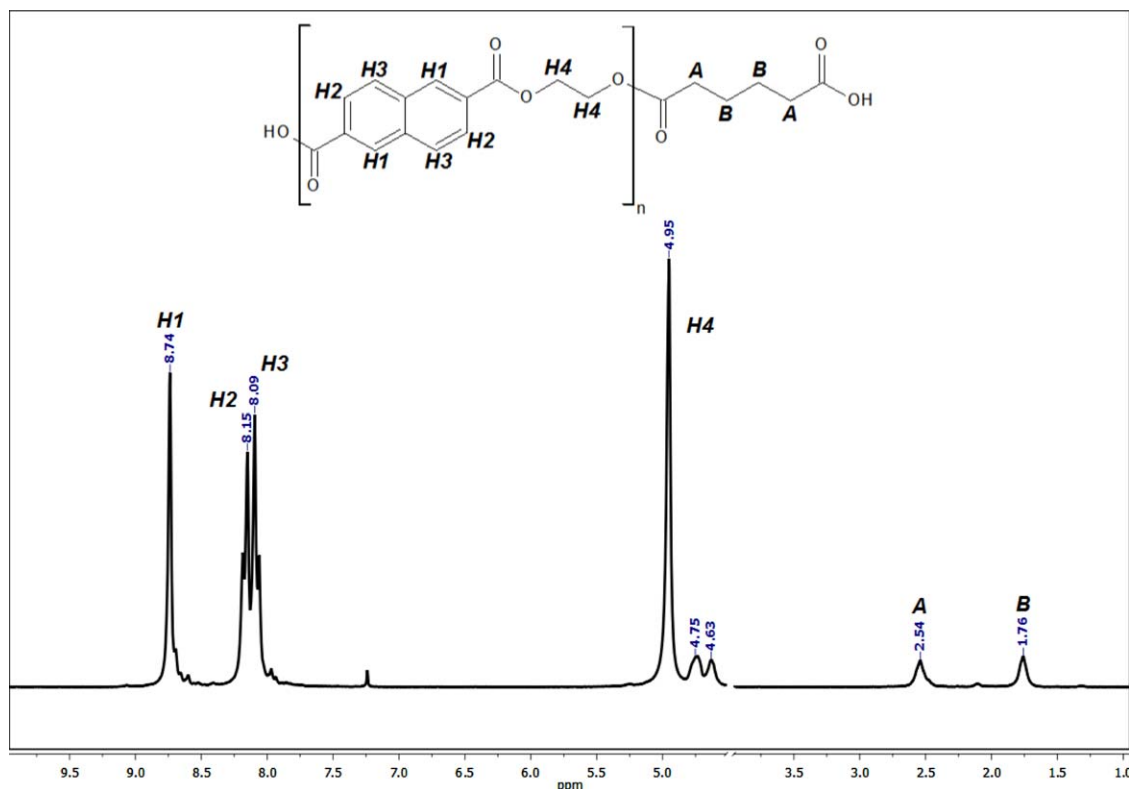


Figure 1. ^1H -NMR-spectrum and peak assignments of the characteristic protons in PEN-oligomer degraded in presence of adipic acid. [Color figure can be viewed in the online issue, which is available at wileyonlinelibrary.com.]

be explained by the reaction of adipic acid with terminal hydroxyl-groups and by chain scission caused by the acid through cleavage of ester-linkages. This confirms the NMR results and, hence, provides further experimental support that chemical degradation of PEN to oligomers had taken place under concomitant formation of blocked end groups.

In the finger print region, the absorbance band of the $\text{C}=\text{O}$ ester-bond at 640 cm^{-1} (Table IV, Figure 4) has lost significantly in intensity in the spectra of the oligomeric sam-

ples. The decrease in the absorbances at 2899 and 2963 cm^{-1} , which are characteristic for the $-\text{CH}_2-$ stretching vibrations (ν) of the ethylene-bridge implies that bond scission of the ethylene bridge has occurred to a significant extent. Moreover, the reduced intensity of the $\text{C}-\text{O}-\text{C}$ deformation vibration at 640 cm^{-1} shows directly the cleavage of ester-bridges during oligomer formation and, hence, provides indirect support of the observed decrease in molecular weight of the polyester samples by adipic acid treatment.

Table III. Chemical Shifts of Pure PEN, Adipic Acid, Oligomeric Degradation Products, Peak Areas of Characteristic Protons, Number-Average Molecular Weights M_n , Calculated and Resulting Degrees of Polymerization of the Degraded Products

Sample	Chemical shift δ (ppm)						Peak area		M_n (g mol^{-1})	Calculated DP ^a	Experimental DP ^b
	H1	H2	H3	H4	A	B	H4	B			
PEN	8.71	8.12	8.07	4.92–4.74	-	-	-	-	-	-	-
O1	8.74	8.16	8.10	4.96–4.63	2.55	1.76	5.20	1.00	1211	5	5
O2	8.75	8.16	8.11	4.95–4.63	2.54	1.76	11.20	1.00	2665	10	11
O3	8.73	8.14	8.09	4.94–4.61	2.53	1.74	20.01	1.00	4845	20	20
O4	8.75	8.16	8.11	4.96–4.64	2.34	1.56	42.21	1.00	10,174	40	42
O5	8.73	8.14	8.09	4.94–4.64	2.53	1.75	78.27	1.00	18,894	78	78
O6	8.76	8.17	8.12	4.97–4.64	2.55	1.71	160.01	1.00	38,757	158	160
Adipic acid	-	-	-	-	2.56	1.77	-	-	-	-	-

^aPredicted DP according to Geyer et al.²⁶

^bDP as obtained from NMR-measurements.

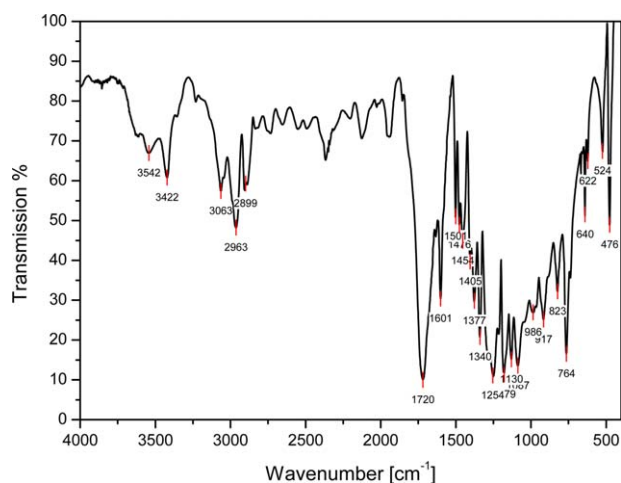


Figure 2. Infrared spectrum of pure PEN. [Color figure can be viewed in the online issue, which is available at wileyonlinelibrary.com.]

Thermal Properties of PEN Oligomers

The PEN fragments obtained from adipic acid treatment were characterized by DSC experiments to investigate the thermal properties of the resulting oligomeric samples in dependence of their degree of degradation.³⁹ The resulting melting temperatures (as determined from the peak minima observed in the thermograms from the second heating cycle) and reaction enthalpies as well as crystallization temperatures and crystallization enthalpies of each sample are summarized in Table V. The thermal properties were correlated with the DP that was quantified using the NMR-measurements.

With decreasing amount of adipic acid and hence increasing DP, the melting temperatures of the oligomeric samples show an increase in temperature from 227 to 268°C (Figure 5), the melting temperature of original PEN. Within this range, samples of lower DP can be clearly distinguished, since their melting temperatures differ clearly from each other (O1, O2, O3, and Table V). In contrast, samples of higher DP and thus higher molecular weight have much less difference in melting temperature and converge asymptotically to the melting temperature of untreated PEN. Obviously, the size of oligomers can be correlated to the melting behavior, especially in case of lower molecular weights. However, it is experimentally difficult to distinguish between high molecular weight polymers because their melting properties are less distinctly different (Table V).

The oligomer size is also reflected by the reaction enthalpies (Table V). With decreasing concentration of scission agent and thus growing DP, the reaction enthalpies increase from $\sim 26 \text{ J g}^{-1}$ (O1, Table V) to 52 J g^{-1} of untreated PEN. Again, oligomers with lower molecular weight (O1, O2 and O3) have greater differences in reaction enthalpy, allowing these samples to be distinguished more easily from each other based on reaction enthalpy. However, the differences in reaction enthalpies of the higher molecular weight samples (O5 and O6) are less distinct and show an asymptotic behavior towards the reaction enthalpy of original PEN.

The crystallization temperatures show the same behavior as the melting temperatures. Crystallization temperatures increase with higher DP (Table V). Samples with lower molecular weight (O1, O2, and

O3) exhibit a greater difference in crystallization temperature, whereas the temperature differences are much less pronounced for the oligomeric samples of higher molecular masses (O4, O5, and O6).

It is noteworthy, that for pure PEN no crystallization peak was found in the cooling segment even at a low cooling rate of 2 K min^{-1} after heating. Under such conditions, crystallization should be readily observed. However, no crystallization peak was found in our case although in the literature a crystallization temperature range from 210–220°C depending on the molecular weight is reported for PEN.^{19,40} Since in the heating segment of the DSC experiment a broad melting range was detected it is nevertheless concluded that PEN was not in an amorphous but a semicrystalline state (Figure 5).

The reason for the missing crystallization peak was the relatively low amount of 10 mg of PEN sample used. When the DSC experiment was performed again using 35 mg of sample (data not shown), a small crystallization peak was visible in the cooling segment. When PEN crystallization was performed from solution in hexafluoroisopropanol upon evaporation of the solvent an even more pronounced signal was observed. A possible reason for the experimental difficulty in observing crystallization in DSC could be the chemical structure of the repeating unit ethylene naphthalate in combination with a high DP of

Table IV. Assignments of IR-Absorbances of PEN

Wavenumber (cm^{-1})	Assignment ^{a,b,c,d,e}
3542	ν (OH)
3422	Overtone (C=O)
3063	ν (aromat. CH)
2963	ν_{as} (CH_2) amorph
2899	ν_{s} (CH_2) cristallin
1720	ν (C=O)
1601	Aromat. Ring vibration
1501	Aromat. Ring vibration
1476	d (CH_2) trans
71,454	d (CH_2) gauche
1405	Aromat. Ring vibration
1377	γ (CH_2) gauche
1340	γ (CH_2) trans
1254	ν (=C–O) + aromat
1179	Naphthalene ring vibration
1130	Naphthalene ring vibration
1087	ν_{s} (O–C) gauche
917	(O=C–O)
764	d (aromat. CH out of plane)
640	d (aromat. CH out of plane)
476	d (aromat. CH out of plane)

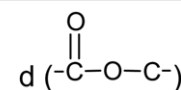
^a ν : stretching vibration.

^b ν_{as} : asymmetrical stretching.

^c ν_{s} : symmetrical stretching.

^d d : in-plane deformation vibration.

^e γ : out-of-plane deformation vibration.^{37,38}



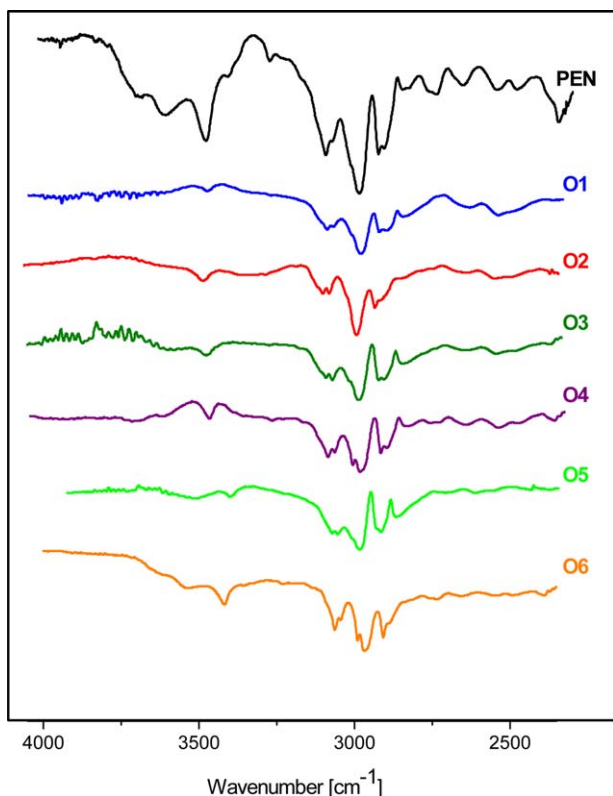


Figure 3. Infrared spectrum in the wavenumber range from 3750 to 2750 cm^{-1} of PEN polymer and the oligomeric reaction products O1 to O6. [Color figure can be viewed in the online issue, which is available at wileyonlinelibrary.com.]

PEN. The inherent immobility of PEN molecular chains might reduce the speed of crystallization during the cooling segment of the thermal measurement.^{40–42}

In Table V, the crystallinities of the oligomeric samples are given as calculated from the reaction enthalpies.^{39,43} As expected, the degree of crystallization increases with increasing sequence length and is highest for the parent polymer PEN.

Treatment with adipic acid leads to a reduction in chain length, thereby rendering the resulting oligomeric products more mobile and enabling them to crystallize during the cooling phase of the DSC experiment. This is visible in the thermogram as an additional crystallization peak. The crystallization temperature shows an increase with increasing DP.

The observed trend in crystallization enthalpies also indicates that PEN-oligomers with different molecular weights were successfully synthesized (Table V). Enthalpies of crystallization increase with growing chain length of the oligomers O1 to O6. Again, oligomers generated by higher concentrations of adipic acid (O1, O2, O3, and Table V) have greater differences in crystallization enthalpies. These enthalpy differences decrease from O3 to O6 in an asymptotic manner.

Synthesis of co-Polyesters from Oligomeric PEN and PET

Characterization of Sequence Length. Block-*co*-polyesters were synthesized from PEN and PET oligomers. The applied PEN oligomers were produced by treating PEN with different con-

centrations of adipic acid in the melt under inert gas atmosphere (Section “Synthesis of Oligomers,” Table I). The oligomeric PET building blocks were prepared in an analogous way as described in Geyer et al.²⁶ Table V shows some characteristic thermal properties of the PET building blocks used for tailoring the PET-PEN block-*co*-polymers.

PEN- and PET-oligomers of different sequence length combinations (see experimental design, Table II) were melt-mixed under nitrogen atmosphere to obtain block-*co*-polyesters containing defined segments (Table II). For each oligomer composition, a reference experiment was conducted using extended mixing times with the aim of producing random-*co*-polyesters. Prolonged melt-mixing of PET and PEN species leads to the formation of random-*co*-polyesters due to the advancing of the transesterification reaction until an equilibrium is reached.⁴⁴ The random-*co*-polyesters were synthesized to analyze whether the defined nature of block-*co*-polyester architecture lead to significant differences in the surface energetic and thermal properties of the resulting materials.

The average number of repeating units of each polyester species comprising the *co*-polyester is denoted as the block length of each respective polyester species. Block lengths of both block- and random-*co*-polyester samples were determined by evaluating the extent of transesterification as determined by NMR spectroscopy.⁴⁴

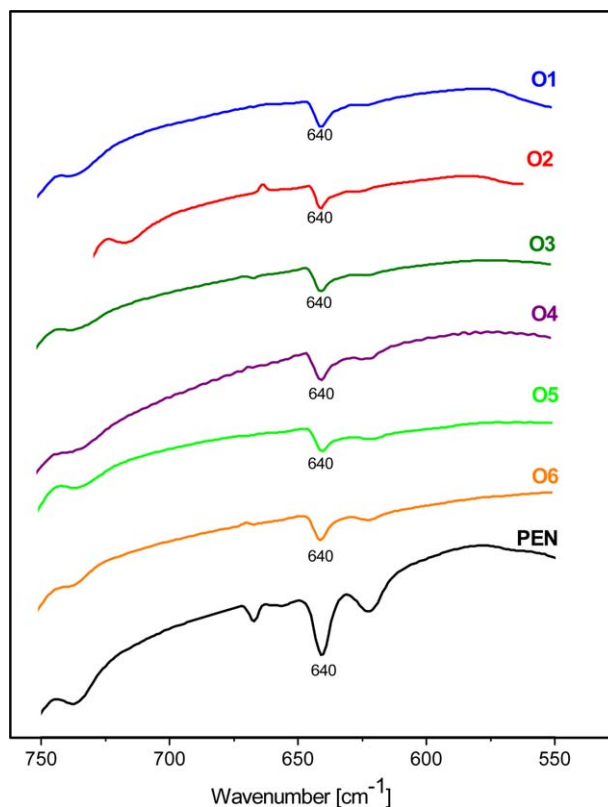


Figure 4. Infrared spectrum in the wavenumber range from 750 to 550 cm^{-1} of PEN polymer and the oligomeric reaction products O1 to O6. [Color figure can be viewed in the online issue, which is available at wileyonlinelibrary.com.]

Table V. Correlation of the Degree of Polymerization with Melting Peaks, Reaction Enthalpies, Crystallization Peaks, Crystallization Enthalpies, and Crystallinity

Sample	DP ^a	T _m ^b (°C)	ΔH _m ^c (J g ⁻¹)	T _c ^d (°C)	ΔH _c ^e (J g ⁻¹)	X _c (%) ^f
O1	5	227	26	193	19	26
O2	11	241	32	206	32	32
O3	20	253	39	215	37	38
O4	42	258	41	221	39	40
O5	78	256	42	223	40	40
O6	160	262	44	225	42	43
PEN	228	268	52	-	-	50
PET5	5	213	42	165	38	30
PET20	20	248	51	208	49	36
PET40	40	252	54	213	51	39

^a Degree of polymerization.^b Melting temperature.^c Reaction enthalpy.^d Crystallization temperature.^e Crystallization enthalpy.^f Crystallinity calculated according to Pielichowski.^{39,43}

The block lengths of PET segments (LnPET) and PEN segments (LnPEN) in the novel co-polyesters were calculated from the areas of the ethylene peaks in the ¹H-NMR-spectra originating from the ethylene units of PET (*A*_{TET}, peak G, Figure 6), of PEN [integrated intensity of ethylene units from PEN (*A*_{NEN}, Peak A, Figure 6)] and of ethylene units between terephthalic and naphthalic units (*A*_{NET}, peak E, Figure 6) [eqs. (11) and (12)]:⁴⁴

$$\text{LnPET} = \frac{A_{\text{NET}} + 2A_{\text{TET}}}{A_{\text{NET}}} \quad (11)$$

$$\text{LnPEN} = \frac{A_{\text{NET}} + 2A_{\text{NEN}}}{A_{\text{NET}}} \quad (12)$$

In Figure 6, the structural formula of a typical PEN-PET-co-polyester is depicted, showing the specific positions of characteristic ethylene bridges that were used for analysis. In position A are aliphatic protons of an ethylene naphthalate repeating unit, position G represents aliphatic protons of an ethylene terephthalate repeating unit and position E marks ethylene protons linking two different repeating units with each other.

Figure 6 shows the NMR-spectra of a typical block- and a typical random-co-polymer originating from PEN- and PET-oligomers. The segment lengths and degrees of randomness determined from NMR are listed in Table VI.

Figures 6 and Table VI show that the peak intensities of ethylene protons (peak E, Figure 6) that are situated between an ethylene naphthalate and an ethylene terephthalate unit are always lower than the peak intensities of protons from ethylene bridges of PEN- and PET-repeating units. In case of block-co-polyester synthesis, the evaluation of peaks E (characteristic for transesterification) revealed that the application of PEN- and PET-oligomers as tailored building blocks leads to block-co-polyesters of defined PEN and PET sequence compositions. As is clearly seen from Table VI, the synthesized block-co-polyester samples have a block sequence length that corresponds very well

with the segment dimensions of the employed raw materials without significant deviations.

However, the reference co-polyester samples of same compositions that were subjected to prolonged reaction times showed a completely different behavior. In these cases, the relative proportions of peak intensities of ethylene protons between PEN- and PET-segments (Figure 6, Peak E) to the neighboring ethylene protons of PEN- and PET-repeating units (Figure 6, Peak A and G) are reversed (Table VI, samples P6–P10). This time the peaks E (Figure 6) that are characteristic for the transesterification are greater than the adjacent peaks A and G. These samples have much shorter block lengths than the applied

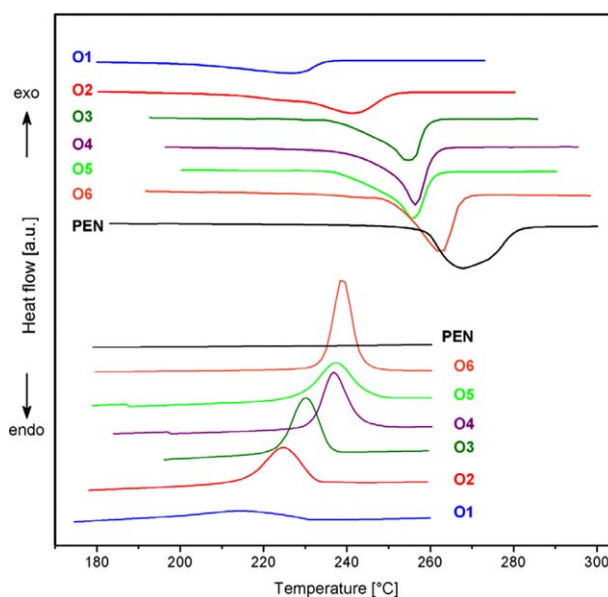


Figure 5. DSC-endotherms and -exotherms of oligomeric PEN-samples including parent PEN. [Color figure can be viewed in the online issue, which is available at wileyonlinelibrary.com.]

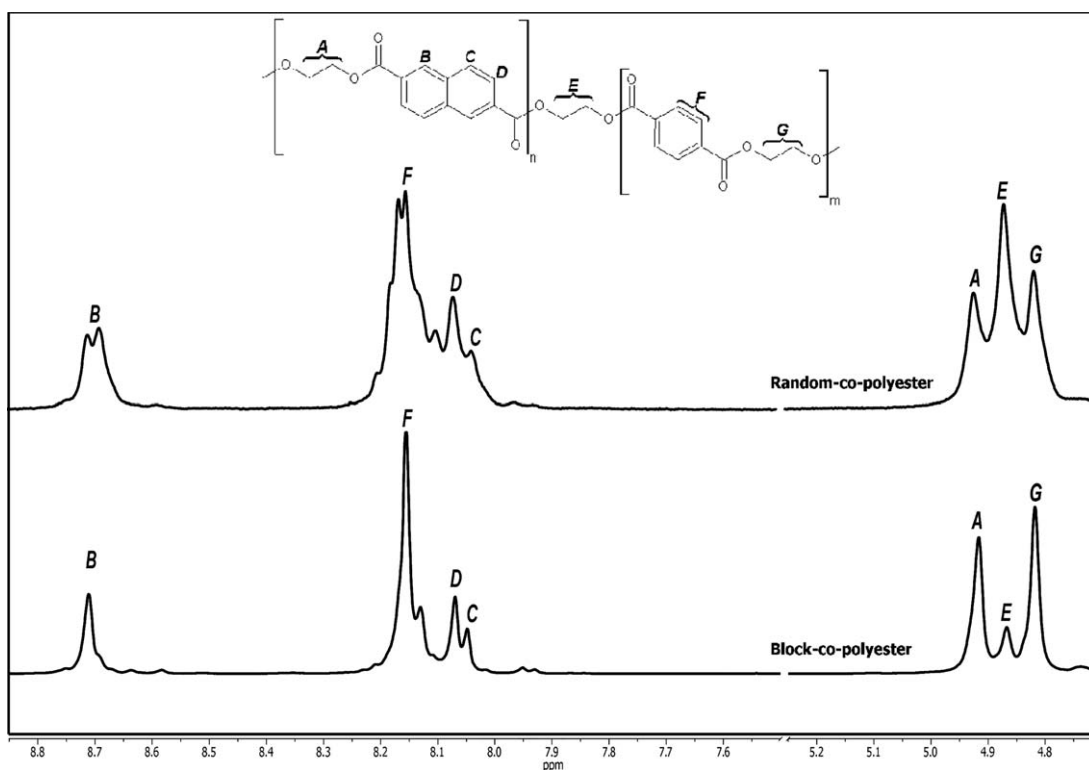


Figure 6. $^1\text{H-NMR}$ -spectrum and peak assignments of characteristic protons of the block-*co*-polyester P2 and the random-*co*-polyester P7. Depicted is the characteristic difference of resonances of ethylene protons (A, E, G) of block versus random-*co*-polyester.

oligomeric components; nearly every sample exhibits PEN- and PET-sequence lengths of around 1 or 2. This is confirmed by the observation that transesterification leads to co-polymers of decreasing segment lengths with respect to every polyester species involved when the reaction time is increased. An equilibrium is reached after a certain period of time, where no further transesterification can be observed. Hence the lengths of the different polyester

building blocks converges towards a minimum and do not change any more.⁴⁴ The only exceptions from this general observation were the random-*co*-polyesters from the combinations of PET40PEN5 (Table VI, P8, the high-low experiment) and PET5PEN40 (Table VI, P9, the low-high experiment) where the PET-peak G and PEN-peak A, respectively, were still more distinct than the transesterification peak E. However, the resulting block lengths of PEN- and PET-

Table VI. PET-, PEN-Sequences, Degree of Randomness (RD) from the Evaluation of the Integrated Peak Intensities of Ethylene Proton Resonances and Glass Transition Temperatures of PET-PEN Co-polymers

Sample	Co-polymer	Co-polymer Type	A_{PEN}^a	A_{NET}^b	A_{TET}^c	LnPET^d	LnPEN^e	RD^f	T_g^g (°C)
P1	PET5PEN5	Block	1.74	1.00	2.34	5.68	4.48	0.40	59
P2	PET40PEN40	Block	18.91	1.00	18.97	38.94	38.82	0.10	96
P3	PET40PEN5	Block	2.15	1.00	19.40	39.80	5.30	0.21	77
P4	PET5PEN40	Block	18.18	1.00	1.80	4.60	37.36	0.24	102
P5	PET20PEN20	Block	9.83	1.00	9.25	19.50	20.66	0.10	93
P6	PET5PEN5rand	Random	0.56	1.00	0.52	2.04	2.12	0.96	47
P7	PET40PEN40rand	Random	0.43	1.00	0.59	2.18	1.86	0.99	90
P8	PET40PEN5rand	Random	0.11	1.00	4.13	9.26	1.22	0.93	71
P9	PET5PEN40rand	Random	4.57	1.00	0.19	1.38	10.14	0.84	97
P10	PET20PEN20rand	Random	0.50	1.00	0.42	1.84	2.00	1.04	89

^a Integrated peak intensity of ethylene protons of PEN repeating unit (peak A).

^b Integrated peak intensity of ethylene protons between PEN and PET repeating units (peak E).

^c Integrated peak intensity of ethylene protons of PET repeating unit (peak G).

^d PET sequence length in co-polyester.

^e PEN sequence length in co-polyester.

^f Degree of randomness.

^g Glass transition temperature.

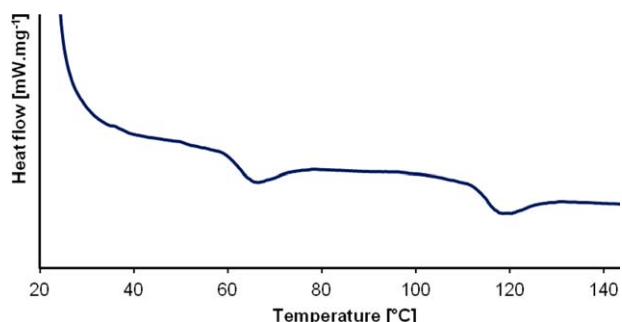


Figure 7. DSC-thermogram showing the blend of PET40 and PEN40. [Color figure can be viewed in the online issue, which is available at wileyonlinelibrary.com.]

domains in the obtained co-polyesters are much shorter in comparison to the initial oligomers PEN40 and PET40, where the component with 40 repeating units decreased to ~ 10 units and the other component (having initially 5 units) to about 1 unit. This can be explained by the great difference of the degrees of polymerization between the two oligomeric polyesters used in each sample. Here, the longer oligomeric component could have reached an equilibrium at about 10 repeating units.

Further evidence for successful tailoring of block-co-polyesters is given by the degree of randomness (RD). The degree of randomness provides information on the architecture of a co-polymer. RD indicates the statistical distribution of the PET- and PEN-sequences in the polymer chain. The RD can be derived from the sequence lengths of the PET- and PEN blocks in the PET-PEN co-polyester. It was calculated from the $^1\text{H-NMR}$ data as the sum of the reciprocal values of PET- and PEN-block lengths [eq. (13)]:

$$\text{RD} = \frac{1}{\text{LnPET}} + \frac{1}{\text{LnPEN}} \quad (13)$$

In the case of a strictly alternating co-polymer, the RD is 2, whereas for a random-co-polymer the RD = 1. Physical blends

of two polymers have an RD close to zero.⁴⁴ For co-polyesters, the degree of randomness can take on values between 0 and 1.

The NMR-measurements showed that the degree of randomness is close to zero for the intended block-co-polyester samples (Table VI). The actual degrees of randomness were all between 0.10 and 0.40 (P1–P5), showing that the produced samples were neither random nor alternating co-polyesters and could, in principle be either block-co-polyesters with tailored block lengths or physical blends. The NMR data suggest the presence of co-polyesters.

NMR measurements of the samples with extended reaction time yielded a degree of randomness in a range from 0.82 to 1.04 (Table VI, P6–P10). This indicates the presence of statistically distributed ethylene naphthalate and ethylene terephthalate units, or, in other words means that there are many ethylene bridges linking a naphthalate and terephthalate unit to each other. Thus, the samples with a degree of randomness close to 1 must be random-co-polyesters.

Characterization of Polymer Phase Composition. The degree of randomness is < 1 ($0 < \text{RD} < 1$) for both block-co-polymers and physical blends of two polymers. Thus, to decide whether the prepared co-polyesters were either physical blends or block co-polymers, all samples were subjected to DSC. Since a physical blend of immiscible polymers like PET and PEN^{17,45–47} is expected to yield two glass transition temperatures (one for each blended component), the presence of only one phase transition should provide proof that actual block- and random-co-polymers have formed. All thermograms contained only a single glass transition (given in Table VI) as was expected in the presence of block- and random-co-polyesters. However, some polymer blends may also show only single glass transitions. This is the case, for instance, when miscible or partially miscible polymers are blended or when the difference in glass transition temperatures of the blend components are small. Therefore, an additional DSC experiment was performed on a blend of PET

Table VII. Dispersive Surface Energies and Specific Desorption Energies for Different Polar Probes of all Co-polyester Samples

Sample	Co-polymer	Co-polymer type	γ_s^D ^a (mJ m ⁻²)	ΔG_{sp} ^b (mJ m ⁻²)					$\frac{\Delta G_{sp}(\text{Dioxane})}{\Delta G_{sp}(\text{Chloroform})}$
				Chloroform	Acetone	1,4-Dioxane	Ethyl acetate	1-Butanol	
P1	PET5PEN5	Block	52.26	27.30	52.57	67.11	61.65	58.59	2.46
P2	PET40PEN40	Block	46.54	23.40	47.41	61.81	57.64	58.14	2.66
P3	PET40PEN5	Block	43.11	22.35	44.30	59.46	53.73	54.78	2.52
P4	PET5PEN40	Block	51.83	26.87	53.87	67.54	63.03	61.20	2.64
P5	PET20PEN20	Block	49.00	24.94	50.31	64.07	59.72	58.34	2.57
P6	PET5PEN5rand	Random	49.98	28.36	52.99	68.60	61.79	61.60	2.42
P7	PET40PEN40rand	Random	48.87	25.62	51.67	65.40	60.55	64.07	2.56
P8	PET40PEN5rand	Random	48.82	25.32	50.94	65.00	62.04	62.23	2.51
P9	PET5PEN40rand	Random	49.38	26.77	52.95	67.28	62.84	66.26	2.55
P10	PET20PEN20rand	Random	49.84	26.77	53.25	66.72	62.16	62.88	2.49

^a Dispersive surface energy [eq. (2)].

^b Specific desorption energy [eq. (3)].

Table VIII. ANOVA Results (Partial Sum of Squares) for the Response Surface Analysis of the Response γ_S^D , ΔG_{sp} (Ethyl Acetate) of Block-*co*-Polyester Samples

	γ_S^D		ΔG_{sp} (ethylacetate)	
	F	P>F	F	P>F
Model	25.32	0.0003	59.81	< 0.0001
[A]	49.18	0.0001	106.36	< 0.0001
[B]	1.59	0.2426	13.90	0.0058
Lack of fit	1.11	0.4611	1.87	0.2789

[A] effect of PET sequence and [B] effect of PEN sequence.

and PEN oligomers (Figure 7). Figure 7 shows that when actual blends were subjected to DSC two clearly separated glass transition temperatures are observed.

The sequence lengths, degrees of randomness and glass transition temperatures of all *co*-polyester specimens are summarized in Table VI. The degrees of randomness for the block-*co*-polyester specimens (Table VI) suggest that presence of mere physical blends can be excluded.^{31,48,49} This supports the NMR-results that had already indicated formation of actual block-*co*-polymers of tailored sequence lengths.

All glass transition temperatures of the block-*co*-polyesters were higher than those of the randomized polymers (Table VI). This observation is in good agreement with the literature. It was shown earlier that block-*co*-polymers have superior thermal stability as reflected by higher melting temperatures and higher glass transition temperatures.^{50–53}

Surface Properties of *co*-Polyesters as a Function of Sequence Length

The target response for the experimental design was the interfacial behavior of the block- and the random-*co*-polymers as expressed by their dispersive surface energy, specific desorption energy, and the Lewis acid base properties. The interfacial properties were determined by IGC.²⁵ The pulverized *co*-polymers were measured twice for statistical reasons. The experimentally determined physicochemical data from IGC are listed in Table VII and provide the basis for RSM.

As seen from Table VII, the ratios of specific desorption energies from 1,4-dioxane and chloroform are in the range from 2.42 to 2.66 without significant difference for both polymer types indicating an acidic surface for block-*co*-polyesters as well as random-*co*-polyesters. This indicates that Lewis acid base properties of these *co*-polymers are not suitable to distinguish between the block- and random-character. Furthermore, it is not possible to adjust the acid base characteristics of the block-*co*-polyesters in dependence of segment compositions.

Response surface methodology is a powerful tool to describe the relationship between several explanatory variables or factors x_i and one or more response variables y . Response surface methodology was applied to show the dependence of interfacial properties on the sequence composition of block-*co*-polyester and to predict the values of selected properties of block-*co*-poly-

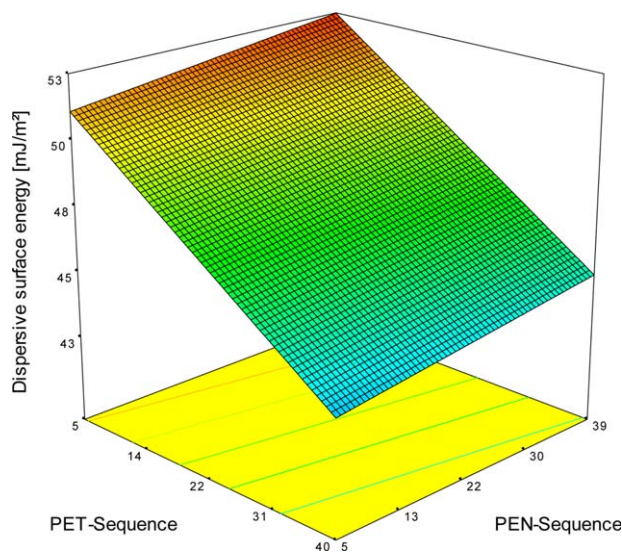


Figure 8. RSM calculated from the ANOVA of dispersive surface energy of block-*co*-polyesters consisting of different block length compositions. [Color figure can be viewed in the online issue, which is available at wileyonlinelibrary.com.]

esters by a regression model. Results of the analysis of variance (ANOVA) for the dispersive surface energy and specific desorption energy towards ethyl acetate as the polar probe are listed in Table VIII. The statistical details for the other used probes regarding models, model accuracies, and factor significances were similar (data not shown).

The $P > F$ -value was used to estimate the statistical significance of the models and factor effects. This value is the probability of observing a factor effect under the assumption that there is no factor effect. In other words, small values of $P > F$ indicate that the corresponding term has a significant effect on the response.

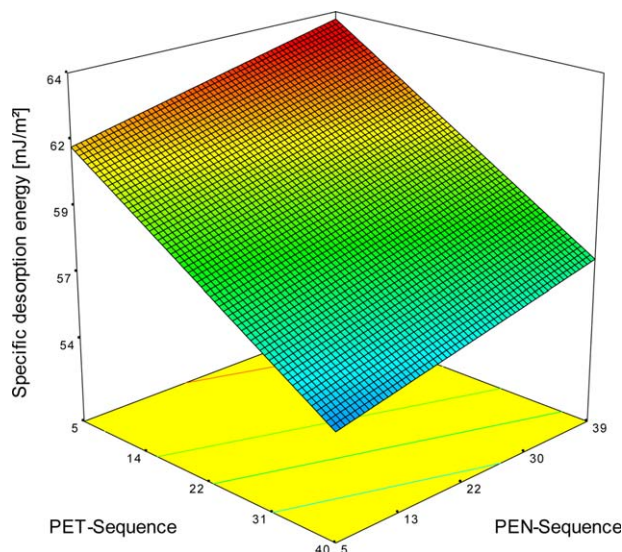


Figure 9. RSM calculated from the ANOVA of specific desorption energy (referring to ethyl acetate) of block-*co*-polyesters consisting of different block length compositions. [Color figure can be viewed in the online issue, which is available at wileyonlinelibrary.com.]

Table IX. ANOVA Results (Partial Sum of Squares) for the Response Surface Analysis of the Response γ_S^D , ΔG_{sp} (Ethyl Acetate) of Random-*co*-Polyester Samples

	γ_S^D		ΔG_{sp} (ethylacetate)	
	F	P>F	F	P>F
Model	6.67	0.0198	12.13	0.0038
[A]	8.13	0.0214	0.0013	0.9716
[B]	5.05	0.0548	24.26	0.0012
Lack of Fit	2.91	0.1307	0.0430	0.9583

[A] effect of original PET sequence and [B] effect of original PEN sequence.

The *F*-value represents an alternative statistical value to judge the significance of the models and analyzed factors. It is calculated by dividing the model mean square by the residual mean squares. Hence, a small error (residual mean square) leads to a respective large *F*-value indicating a significant influence of the analyzed terms on the response.

Calculation of the ANOVA for both target values (dispersive surface energy and specific desorption energy) revealed that the used models were statistically significant (Table VIII). Quantitative modeling was conducted using the single effects of the PET-, and the PEN-sequences (linear model), since neither polynomial nor 2FI fitting improved the model accuracy significantly or added explanatory power. Dispersive surface energy and specific desorption energy were described in terms of coded factors by $\gamma_S^D = 48.43 - 3.71[A] + 0.69[B]$ and ΔG_{sp} (ethyl acetate) = $59.21 - 3.34[A] + 1.25[B]$, where [A] is the block length of PET and [B] is the block length of PEN. The correlation coefficients ($R^2 = 0.86$ for dispersive surface energy, $R^2 = 0.94$ for specific desorption energy) and the *P* > *F*-values of the lack of fit for the two responses show that both models are statistically significant and describe the dataset well. For the target response “dispersive surface energy,” only factor [A] has a significant influence on the response because its coded coefficient is much greater than the coefficients of factor [B]. This is also reflected by the statistical relevance of the corresponding *P* > *F*-values. The *P* > *F*-value of factor [A] is 0.0001, whereas the value for [B] is >0.1 (Table VIII). Since values smaller than 0.05 are considered to be statistically significant the response dispersive surface energy can be described mainly by the PET-sequence. The linear model of the dispersive surface energy is visualized in Figure 8. At low level of PEN-sequence length, variation of PET block dimension has a large effect on dispersive surface energy, whereas at high level of PEN-segments this influence is attenuated.

As a representative response surface for all polar probes, the linear model of the specific desorption energy referring to ethyl acetate showed that both the PET and the PEN sequence composition were statistically significant with *P* > *F*-values <0.05 (Table VIII). The corresponding response surface is depicted in Figure 9. Both PET- and PEN-block dimension affect the response. Increasing the PEN and decreasing the PET block lengths in the block-*co*-polyester leads to an increase of the spe-

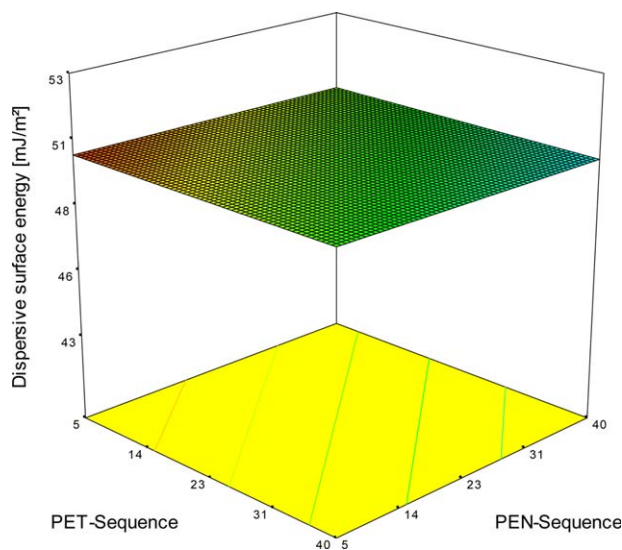


Figure 10. RSM calculated from the ANOVA of dispersive surface energy of random-*co*-polyesters. [Color figure can be viewed in the online issue, which is available at wileyonlinelibrary.com.]

cific desorption energy. Based on the individually adjustable block length composition of block-*co*-polyesters, it is thus possible to regulate the dispersive surface energy and the specific desorption energy of the generated polyesters.

Next, RSM was applied to random-*co*-polyesters. Based on the data of Table VII for random-*co*-polyesters recalculation of the response surface yields the ANOVA given in Table IX.

Both responses were modeled by significant linear models. 2FI and higher polynomial fitting improved neither the model accuracy nor did they add to the explanatory power. In contrast to the defined block-*co*-polyesters, with the random-*co*-polyesters neither the original PET sequence length of the educts (factor [A]) nor the original PEN sequence lengths (factor [B]) were

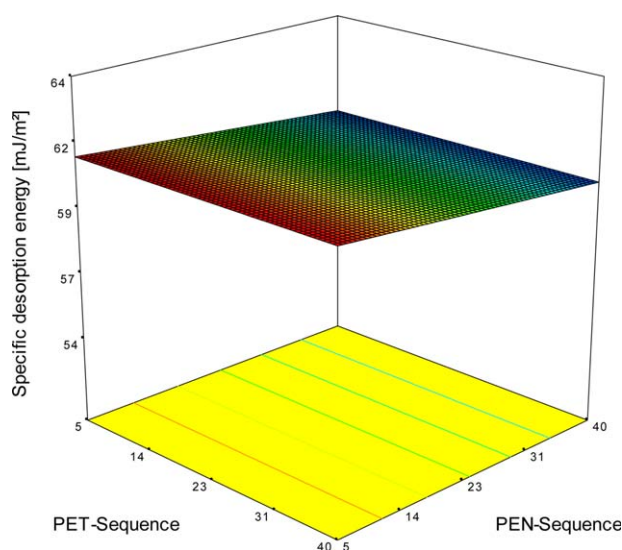


Figure 11. RSM calculated from the ANOVA of specific desorption energy (referring to ethyl acetate) of random-*co*-polyesters. [Color figure can be viewed in the online issue, which is available at wileyonlinelibrary.com.]

Table X. Experimental Settings for the Validation of Calculated RSM and Predicted Values of Dispersive Surface Energy and Specific Desorption Energy for Block-*co*-Polyesters

Sample	Co-polymer	Co-polymer type	LnPET ^a	LnPEN ^b	γ_S^D (mJ m ⁻²)		ΔG_{sp} (ethylacetate) ^d (mJ m ⁻²)	
					Predicted	Measured	Predicted	Measured
P11	PET20PEN5	Block	19.68	4.56	48.32	49.24	58.47	59.44
P12	PET20PEN40	Block	19.62	39.26	49.70	51.09	60.96	61.10
P13	PET5PEN20	Block	5.14	22.06	52.09	52.32	62.49	62.30
P14	PET40PEN20	Block	40.94	18.98	44.37	44.15	55.45	55.48

^aPET sequence length in co-polyester.^bPEN sequence length in co-polyester.^cDispersive surface energy [eq. (2)].^dSpecific desorption energy [eq. (3)].

statistically highly significant as reflected by the $P > F$ values which were both close to 0.05. This is also seen by the model equation $\gamma_S^D = 49.91 - 0.05[A] - 0.04[B]$ describing the response dispersive surface energy, which shows that the intercept is not very much influenced by either changes in factors [A] or [B].

In the model of the specific energy for random-*co*-polyesters only factor [B] was significant whereas the PET sequence length [A] turned out to be statistically not significant (Table IX). A quantitative model was obtained for ΔG_{sp} (ethyl acetate) = $60.55 - 0.003[A] - 0.48[B]$, where [A] is the originally used PET-sequence, [B] is the originally used PEN-sequence.

The $P > F$ value of 0.0198 for the model of the dispersive surface energy and the $P > F$ value of 0.0038 for the model of the specific surface energy are both smaller than the significance level $\alpha = 0.05$. Hence, both models have to be regarded as moderately statistically significant. However, the observed effects are not very pronounced and model accuracies are rather low as reflected by the correspondingly low correlation coefficients ($R^2 = 0.63$ for dispersive surface energy and $R^2 = 0.75$ for specific desorption energy of random-*co*-polyesters). According to the magnitude of coded factor coefficients in both equations it is obvious, that there is no considerable net effect of PET or PEN on neither dispersive nor specific desorption energy, since all coded coefficients are < 1 and hence illustrate the rather negligible effect of each factor. This trend becomes evident in the graphical visualization of the equations (Figures 10 and 11).

A possible explanation could be that independent of the initial PET- and PEN-compositions, during the reaction under prolonged mixing time all employed building blocks are reduced in size until a state of equilibrium is reached. The resulting small units are statistically distributed across the polymer chain leading to a homogeneous distribution of PET- and PEN-monomers in the random-*co*-polyesters. Hence, this randomization in the generated *co*-polyesters leads to a homogenization of the related surface property, and the original molecular weight distribution of the used oligomers is not of importance anymore. Thus by comparison of RSM of interfacial properties for random and block-*co*-polyesters it is apparent, that random-*co*-

polyesters homogenize interfacial chemistry of *co*-polyesters such as dispersive surface energy or specific desorption energy. However, precise tailoring of block length composition in block-*co*-polyesters enables controlling thermodynamic conditions of such *co*-polymers. To verify the predictions of the models for block-*co*-polyesters validation experiments were performed in a final step.

Validation of RSMs. To validate the predictive power of the RSM of dispersive and specific properties of block-*co*-polyesters a series of validation experiments was performed. PET-PEN-*co*-polyesters were prepared with sequence length compositions that were different from the compositions of the block-*co*-polyesters used to generate the RSMs. The actual sequence lengths of the block-*co*-polyesters used for validation were determined by NMR and yielded predictions of values for dispersive and specific surface energies that were verified experimentally by IGC. Table X shows that the predicted and the experimental values were in good agreement.

CONCLUSION

The aim of this study was to demonstrate the rational synthesis of tailored PET-PEN block-*co*-polymers from PET and PEN oligomers of defined chain lengths. The oligomeric building blocks of known degrees of polymerization were accessible from controlled degradation of the parent polymers via a chemical recycling process. A series of block-*co*-polyesters of systematically varied chain segments was successfully prepared from the oligomers. Block-*co*-polyesters and random-*co*-polyester prepared from the same oligomeric materials displayed different behavior with respect to their interfacial properties. It was found that the specific and dispersive surface energies of the block-*co*-polymers could be tuned by variation of the sequence composition. The influence of polymer composition on the interfacial properties was quantified using a RSM approach. RSMs were derived for dispersive and specific surface energies for both *co*-polyester species. Both, the dispersive surface energy and the specific desorption energy were linear proportional to the PET chain length. The PEN chain length was of less importance. However, the Lewis acid and base properties did not

differ for the different block-co-polyesters. Moreover, the Lewis acid and base properties were also not suitable to distinguish between random- and block-co-polyesters. No effect of oligomer sequence length was found for random-co-polyester whereas it was possible by means of individual tailoring block segments in PET-PEN-block-co-polyesters to adapt surface properties. By controlling thermodynamic characteristics of interfacial chemistry in dependence of sequence composition in block-co-polymers technological issues can be addressed more adequately. One potential application of the designed block-co-polymers could be as modifying agents for improving the compatibility of PET/PEN blends.

ACKNOWLEDGMENTS

The authors sincerely thank the project management Jülich, Forschungszentrum Jülich (project number: 17 N18 10) for financial support. They also would like to thank Klaus Albert and his group at the University of Tübingen, Germany for performing the NMR-measurements.

REFERENCES

1. Isayev, A. I. *Encyclopedia of Polymer Blends*; Wiley-VCH: Weinheim, **2010**; Vol. 1.
2. Epel, J. N. In *Engineered Materials Handbook*; ASM International Handbook committee, **1988**; Vol. 2, pp 487, 632.
3. Otley, M. T.; Alamer, F. A.; Zhu, Y.; Singhaviranon, A.; Zhang, X.; Li, M.; Kumar, A.; Sotzing, G. A. *Appl. Mater. Interfaces* **2014**, 6, 1734. doi: 10.1021/am404686w.
4. Kausar, A.; Zulfiqar, S.; Sarwar, M. I. *J. Appl. Polym. Sci.* **2014**, 131, doi: 10.1002/app.39954.
5. Hachemi, R.; Belhaneche-Bensemra, N.; Massardier, V. *J. Appl. Polym. Sci.*, **2014**, 131, doi: 10.1002/app.40045.
6. Freitas, F.; Alves, V. D.; Reis, M. A.; Crespo, J. G.; Coelho, I. M. *J. Appl. Polym. Sci.*, **2014**, 131, doi: 10.1002/app.40047.
7. Mi, H.-Y.; Jing, X.; Salick, M. R.; Crone, W. C.; Peng, X.-F.; Turng, L.-S. *Adv. Polym. Tech.*, **2014**, 33, doi: 10.1002/adv.21380.
8. Hu, J.; Zhang, H.-B.; Hong, S.; Jiang, Z.-G.; Gui, C.; Li, X.; Yu, Z.-Z. *Ind. Eng. Chem. Res.* **2014**, 53, 2270, doi: 10.1021/ie4035785.
9. Sun, Y.-M.; Shieh, J.-Y. *J. Appl. Polym. Sci.* **2001**, 81, 2055.
10. Mohamadi, S.; Sanjani, N. S. *e-Polymers* **2009**, 135, 1.
11. Vaia, R. A.; Krishnamoorti, R. In *Polymer Nanocomposites: Introduction*; Vaia, R. A.; Krishnamoorti, R., Eds.; ACS Symposium Series 804, Washington D.C., **2002**; Chapter 1, p 1.
12. Ji, Q. L.; Zhang, M. Q.; Rong, M. Z.; Wetzel, B.; Friedrich, K. *J. Mater. Sci.* **2004**, 256, 1072.
13. Manias, E.; Touny, A.; Wu, L.; Strawhecker, K.; Lu, B.; Chung, T. C. *Chem. Mater.* **2001**, 13, 3516.
14. Faucheu, J.; Gauthier, C.; Chazeau, L.; Cavaillé J.-Y.; Melon, V.; Pardal, F.; Bourgeat Lami, E. *Polymer* **2010**, 51, 4462.
15. Picken, S. J.; Vlasveld, D. P. N.; Bersee, H. E. N.; Özdilek, C.; Mendes, E. In *Nanocomposites: Ionic Conducting Materials and Structural Spectroscopies*; Knauth, P., Schoonman, J., Eds.; Springer, **2008**; Chapter 4, p 143.
16. Tharmapuram, S. R.; Jabarin, S. A. *Adv. Polym. Tech.* **2003**, 22, 137.
17. Aoki, Y.; Li, L.; Amari, T.; Nishimura, K.; Arashiro, Y. *Macromolecules* **1999**, 32, 1923.
18. Hu, Y. S.; Liu, R. Y. F.; Zhang, L. Q.; Rogunova, M.; Schiraldi, D. A.; Nazarenko, S.; Hiltner, A.; Baer, E. *Macromolecules* **2002**, 35, 7326.
19. Po, R.; Occhiello, E.; Giannotta, G.; Pelosini, L.; Abis, L. *Polym. Adv. Technol.* **1995**, 7, 365.
20. James, N. R.; Ramesh, Ch.; Sivaram, S. *Macromol. Chem. Phys.* **2001**, 202, 2267.
21. Lu, T.-S.; Sun, Y.-M.; Wang, Ch.-S. *J. Polym. Sci. Part A: Polym. Chem.* **1995**, 33, 2841.
22. Jun, H. W.; Chae, S. H.; Park, S. S.; Myung, H. S.; Im, S. S. *Polymer* **1999**, 40, 1473.
23. Khonakdar, H. A.; Golriz, M.; Jafari, S.-H.; Wagenknecht, U. *Macromol. Mater. Eng.* **2009**, 294, 272.
24. Yang, H.; Ma, J.; Li, W.; Liang, B. *Polym. Eng. Sci.* **2002**, 42, 1629.
25. Schreiber, H. P.; Lloyd, D. R. In *Inverse Gas Chromatography Characterization of Polymers and Other Materials*; Schreiber, H. P., Lloyd, D. R., Ward, T. C., Pizaña, C. C., Eds.; ACS Symposium Series 391, Washington D.C., **1989**; Chapter 1, p 1.
26. Geyer, B.; Röhner, S.; Lorenz, G.; Kandelbauer, A. *J. Appl. Polym. Sci.*, **2014**, 131, doi: 10.1002/app.39786.
27. Baldissera, A.; Valério, Carlos E. S.; Basso, Nara R. de S.; Guaragna, F.; Einloft, S.; Tessier, M.; Fradet, A. *Quim. Nova* **2005**, 28, 188.
28. Charlier, Y.; Godard, P.; Daoust, D.; Strazielle, C. *Macromolecules* **1994**, 27, 3604.
29. Li, H.; Jackson, A. B.; Kirk, N. J.; Mauritz, K. A.; Storey, R. F. *Macromolecules* **2011**, 44, 694.
30. Saint-Loup, R.; Robin, J.-J.; Boutevin, B. *Macromol. Chem. Phys.* **2003**, 204, 970.
31. Schultz, J.; Lavielle, L. In *Inverse Gas Chromatography: Characterization of Polymers and Other Materials*; Lloyd, D. R., Ward, T. C., Schreiber, H. P., Pizaña, C. C., Eds.; American Chemical Society: Washington, D.C., **1989**; Vol. 391, Chapter 14, p 185.
32. Lara, J.; Schreiber, H. P. *J. Coat Technol.* **1991**, 63, 81.
33. Khuri, A.; Mukhopadhyay, S. *WIREs Comp. Stat.* **2010**, 2, 128, doi: 10.1002/wics.73.
34. Siebertz, K.; van Bebber, D. In *Statistische Versuchsplanung: Design of Experiments*; Springer: Heidelberg, Dordrecht, London, New York, **2010**; Vol. 1, Chapter 1, p 21.
35. Kessler, W. In *Multivariate Datenanalyse für die Pharma-, Bio- und Prozessanalytik*; Wiley-VCH: Weinheim, **2007**; Chapter 3, p 99.
36. Khuri, A.; Cornell, J. In *Response Surfaces*, 2nd ed.; Dekker: New York, **1996**; Chapter 2.3.

37. Ouchi I.; Hosoi, M.; Shimotsuma, S. *J. Appl. Polym. Sci.* **1977**, *21*, 3445.
38. Berdous S.; Saidi-Amroun, N.; Bendaoud, M. *Int. J. Polym. Anal. Ch.* **2010**, *15*, 54.
39. Pielichowski, K.; Flejtuch, K. *Polym. Adv. Technol.* **2002**, *13*, 690.
40. Buchner, S.; Wiswe, D.; Zachmann, H. G. *Polymer* **1989**, *30*, 480.
41. Keating, M. Y. *Thermochim. Acta* **1998**, *319*, 201.
42. Karger-Kocsis, J.; Moskala, E. *J. Polymer* **2000**, *41*, 6301.
43. Berdous S.; Berdous D.; Saidi-Amroun, N.; Akretche, D. E.; Saidi, M. *Int. J. Polym. Anal. Ch.* **2013**, *18*, 358.
44. Kim, S. H. In *Modern Polyesters*; Scheirs, J., Long, T. E., Eds.; Wiley: Chichester, West Sussex, **2003**; Chapter 20, p 673.
45. Takahashi, M.; Ito, M.; Ida, S.; Ikawa, T. *J. Appl. Polym. Sci.* **2005**, *97*, 2428.
46. Andresen, E.; Zachmann, H. G. *Colloid Polym. Sci.* **1994**, *272*, 1352.
47. Ihm, D. W.; Park, S. Y.; Chang, C. G.; Kim, Y. S.; Lee, H. K. *J. Polym. Sci. Part A: Polym. Chem.* **1996**, *34*, 2841.
48. Yu, S.; Saleh A. J. *J. Appl. Polym. Sci.* **2001**, *81*, 11.
49. Porter, R. S.; Wang, L.-H. *Polymer* **1992**, *33*, 2019.
50. Wang, Z.; Chen, T.; Xu, J. *Polym. Int.* **2001**, *50*, 249.
51. Palermo, E. F.; McNeil, A. J. *Macromolecules* **2012**, *45*, 5948.
52. Liu, R. Y. F.; Hu, Y. S.; Hibbs, M.R.; Collard, D.M.; Schiraldi, D. A.; Hiltner, A.; Baer, E. *J. Polym. Sci. Part B: Polym. Phys.* **2003**, *41*, 289.
53. Kenney, J. F. *Polym. Eng. Sci.* **1968**, *8*, 216.